Systematic microbial production of optically active dissolved organic matter in subarctic lake water

M. Berggren,[a] Gudasz, C.,[b] Guillemette, F.,[c] Hensgens, G.,[a] Ye, L.,[a,d] and Karlsson, J.[b]

[a]Department of Physical Geography and Ecosystem Science, Lund University, Lund, Sweden

[b]Climate Impacts Research Centre (CIRC), Department of Ecology and Environmental Science, Umeå University, Umeå, Sweden

[c]Centre for Research on Watershed - Aquatic Ecosystem Interactions (RIVE), Université du Québec à Trois-Rivières, Trois-Rivières, Québec, Canada

[d]School of Geographic Sciences, Nantong University, Nantong, PR China

Acknowledgements

We thank Karl Heuchel for assistance during sampling. We thank Matthias Siewert for help to construct the land use map. The bacterial production measurements were carried out by Patricia Koch as part of a student internship. The study was funded by the Swedish research council (VR) grant #2016-0527 and the Knut and Alice Wallenberg Foundation grant #2016.0083. MB was supported by the Swedish Research Council for Environment, Agricultural Sciences and Spatial Planning (FORMAS) grants #239-2014-698 and #2017-00772. FG was supported by a Natural Sciences and Engineering Research Council of Canada (NSERC) – Discovery grant.

ABSTRACT

The ecology and biogeochemistry of lakes in the subarctic region are particularly sensitive to changes in the abundance and optical properties of dissolved organic matter (DOM). External input of colored DOM to these lakes is an extensively researched topic, but little is known about potential reciprocal feedbacks between the optical properties of DOM and internal microbial processes in the water. We performed 28-d dark laboratory incubation trials on water from 101 subarctic tundra lakes in northern Sweden, measuring the microbial decay of DOM and the resulting dynamics in colored (CDOM) and fluorescent (FDOM) DOM components. While losses in dissolved oxygen during the incubations corresponded to a 20% decrease in mean DOM, conversely the mean CDOM and total FDOM increased by 22% and 30%, respectively. However, the patterns in microbial transformation of the DOM were not the same in all lakes. Notably, along the gradient of increasing ambient CDOM (water brownness), the lakes showed decreased microbial production of protein-like fluorescence, lowered DOM turnover rates and decreasing bacterial growth per unit of DOM. These trends indicate that browning of subarctic lakes systematically change the way that bacteria interact with the ambient DOM pool. Our study underscores that there is no unidirectional causal link between microbial processes and DOM optical properties, but rather reciprocal dependence between the two.

41 INTRODUCTION

42 Subarctic regions undergo climate related transitions, evident from thawing permafrost
43 (Åkerman and Johansson 2008; Lawrence et al. 2012), changes in treeline limits (Kullman
44 2002) and vegetation succession distributions (Callaghan et al. 2002; Kullman 2014). Many
45 lakes in these regions are at risk of transitioning from a clear-water into a brown-water state
46 because of hydrologically activated soil and peat horizons that leach brown-pigmented
47 dissolved organic matter (DOM) (Jansson et al. 2010; Wauthy et al. 2018). In the aquatic
48 environment, this allochthonous DOM tends to reduce productivity of benthic habitats
49 (Karlsson et al. 2009; Urtizberea et al. 2013), change nutrient supply and food web structure
50 (Berggren et al. 2015; Creed et al. 2018; Jansson et al. 2007), and cause CO_2 outgassing to
51 the atmosphere (Lapierre et al. 2013). The extent of these effects are however difficult to
52 predict due to the complex interactions between DOM and lake ecosystems that tend to result
53 in non-linear responses (Solomon et al. 2015). Nonetheless, it is clear that DOM plays a
54 central role in the climate change impact on lake ecosystem functioning, especially in near-
55 arctic environments which are particularly sensitive to climate-induced changes in the carbon
56 cycle (Vincent et al. 2012).
57
58 The fractions of DOM that are optically active, i.e. the light-absorbing 'colored' (CDOM)
59 and the 'fluorescent' (FDOM components) fractions are relatively persistent in the
60 environment (Berggren et al. 2018; Kellerman et al. 2015), compared to the smaller pool of
61 fast cycled non-colored DOM in freshwaters (Berggren et al. 2010). However, due to their
62 commonly large concentrations, CDOM and FDOM are associated with significant quantities
63 of reactive compounds (Lapierre and del Giorgio 2014; Wetzel 1995), including microbially
64 degradable DOM fractions of importance for the landscape carbon cycling (Lapierre et al.
65 2013). Research on the dynamics of optically active DOM in the arctic and subarctic tundra

regions is limited, but results from boreal and temperate lakes suggest that increasing loading of terrestrially derived CDOM generally causes a shift from fast-cycled low DOM concentrations characterized by protein-like fluorescence (Koehler et al. 2012), to larger and more slowly cycled humic-like DOM pools maintained by hydrological input (Guillemette and del Giorgio 2011). However, total amounts of reactive and protein-like DOM may increase with CDOM on large scales, because even if such fractions may represent relatively small parts of the terrestrially derived DOM, this is eventually outweighed by the high total DOM concentrations in brown lakes (Lapierre and del Giorgio 2014).

Optically active organic constituents are not only imported from the catchment, but also produced by microbial processing of autochthonous (i.e. algal derived) DOM (Romera-Castillo et al. 2011). Aquatic microbial production of CDOM is evident from laboratory (Shimotori et al. 2009; Tranvik 1993) and marine (Rowe et al. 2018) studies, but corresponding observations in natural freshwaters are scarce. In brown-water lakes, CDOM tends to be consumed by bacteria faster that it is produced (Berggren et al. 2018). Regarding FDOM, a study of lakes and streams in southern Québec (Guillemette and del Giorgio 2012) found that most fluorescence components were net produced in clear-water systems where significant fractions of the DOM were of autochthonous origin, whereas in systems dominated by allochthonous DOM the FDOM tended to be net consumed. In clear-water alpine lakes, production of protein-like fluorescence has been observed after algal blooms (Miller and McKnight 2010), attributed to nitrogen accumulation in the DOM pool (Goldberg et al. 2015). This agrees with experimental results confirming FDOM production, especially protein-like fluorescence, in response to bacterioplankton use and transformation of algal DOM (Fox et al. 2017). However, patterns in microbial net production or consumption of CDOM and FDOM in subarctic lakes remain unexplored.

A dramatic increase in allochthonous DOM (i.e. lake browning) has recently been observed in many arctic lakes (Wauthy et al. 2018), with anticipated impacts on lake carbon balances (Lapierre et al. 2013) as well as food webs (Creed et al. 2018; Williamson et al. 2015). However, little is known about the interaction between lake browning and the balance between internal microbial production and degradation of optically active constituents. Such interactions, which are non-linear by nature (Berggren et al. 2018), can potentially exacerbate or dampen the terrestrial influence on the optical environment in lakes with even small changes, thus influence a wealth of ecological and biogeochemical processes.

Here we hypothesized that due to the natural clear-water state of subarctic tundra lakes, with relatively small inputs of CDOM from terrestrial sources, FDOM is net produced by bacterioplankton, similar to what has been observed in temperate and alpine clear-waters based on algal-derived DOM (Guillemette and del Giorgio 2012; Miller and McKnight 2010). However, we expected that with increasing ambient CDOM the balance between production and consumption of FDOM could switch to net consumption. Moreover, we expected a shift from highly reactive protein-like DOM to more recalcitrant and humic-like DOM along the gradient of increasing CDOM. We tested these ideas by combining a large survey sampling of 101 subarctic lakes in northern Sweden with 28-d laboratory incubation experiments, during which we measured bacterial production and respiration rates and followed changes in the microbial production or consumption of optically active compounds.

112 METHODS

113 *Study area, sampling and site selection*

114 Sampling was carried out west of Abisko, Northern Sweden, in a subarctic mountainous
115 plateau (Fig. S1). The area is characterized by the transition between tundra (Virtanen et al.
116 2016) and Nordic mountain birch forest (Wielgolaski 2005). A map and information on the
117 relative contribution of the land use types in the area is available in Fig. S2. The mean annual
118 temperature and precipitation for the 1970-2000 period (Hijmans et al. 2005) for the study
119 lakes ranged between -0.1 and -1.4 °C, and from 477 to 873 mm respectively along a gradient
120 from east to west. The permafrost conditions of the region is characterised by sporadic and
121 discontinuous permafrost (Brown et al. 1997), with isolated pockets of permafrost in the
122 study catchments (Gisnås et al. 2017).

123

124 In autumn (September 20th, 2017) we carried out a helicopter survey of 149 lakes sampled
125 within 5 h. We used the Eurocopter EC-120B helicopter equipped with special floats, and
126 modified to allow sampling through a trap in the floor within seconds upon landing on the
127 lake surface. This aircraft is the same as that used to carry out the Swedish national lake
128 monitoring program, which samples ca 1000 lakes per year for analysis of water chemical
129 and optical characteristics. Lake water was collected from 1 m depth using a 1.5 L water
130 sampler (UWITEC) pre-rinsed with 10% HCl and Milli-Q water. The turbulence caused by
131 the helicopter upon landing may have induced water mixing to a degree. However, the impact
132 of such mixing on the samples was assumed to be negligible because the lakes were already
133 well mixed, without thermal stratification, on the sampling date. Moreover, the sampling
134 point beneath the helicopter's body is the place with the least turbulence within the
135 helicopter's footprint. Recorded video footage, showing the relatively limited rotor
136 downwash effects around the helicopter, will be shared with readers upon request.

137

138 Samples were transported cold to the laboratory in acid-washed 700 ml polycarbonate bottles,
139 and then further subsampled. Subsamples of water for decay experiments and analyses of
140 optical characterizations were filtered using pre-combusted (4h at 500°C) glass fibre filters
141 (Whatman GF/F), and stored cold in 250 ml acid-washed high-density polyethylene
142 (Nalgene) bottles in a cold room at a constant temperature of 2 °C for a total of 40 days (since
143 sampling) before initiation of the experiments. Preservation of the DOC during storage was
144 optimized by the combination of using burnt GF/F filters, which have less than half pore-size
145 diameter compared with non-combusted GF/Fs thus removing more of the bacteria (Nayar
146 and Chou 2003), and using a storage temperature close to the freezing point. Unfiltered water
147 subsamples for total phosphorus (TP) and total nitrogen (TN) were frozen at -20°C until
148 analysis, while samples for dissolved organic carbon (DOC) were filtered (Whatman GF/F)
149 and acidified with HCl to pH 2. The preserved DOC and nutrient samples were analyzed
150 during spring 2018.

151

152 In total 101 of the sampled sites were selected for this study (Table 1). We selected only sites
153 with *in situ* DOC concentrations above 1.0 mg L^{-1}, due to the general difficulty of measuring
154 the turnover of small carbon pools with acceptable accuracy using standard techniques
155 available to us (Jennings et al. 2018). Additionally, sites were excluded if data records were
156 incomplete or if the specific ultraviolet absorption of DOC at 254 nm ($SUVA_{254}$; decadic
157 absorbance coefficient divided by DOC concentration) was anomalously high indicating that
158 constituents other than DOC, although not measured (e.g. iron), contributed to the optical
159 characteristics of the water (Poulin et al. 2014; Weishaar et al. 2003). We chose the threshold
160 value for accepted *in situ* $SUVA_{254}$ of 6 L mg^{-1} m^{-1}. However, since it is in the nature of
161 $SUVA_{254}$ to have relatively large error variability at low DOC concentrations, the higher

threshold of 8 L mg^{-1} m^{-1} was used for $SUVA_{254}$ values calculated at the end of the decay experiment when DOC had decreased and thus $SUVA_{254}$ uncertainty had increased.

Dissolved organic carbon decay

Decay experiments were carried out in standard dark 20°C conditions, during which the DOC decay with microbial re-growth communities (ambient bacteria that passed through the GF/F filtration) was assessed in parallel with bacterial production (BP) measurements. The DOC loss was inferred from dissolved oxygen (DO) loss using a conversion factor (i.e., the respiratory quotient 'RQ') of 1.0 mole of DOC lost per mole of O_2, which is lower than the average RQ reported for net heterotrophic boreal and temperate lakes but a reasonable assumption for lakes with low terrestrial influence (Berggren et al. 2012).

For each lake water sample, simultaneous and continuous analysis of DO was carried out in duplicate or triplicate 5 ml sensor vials with butyl rubber septa screw caps using a SensorDish Reader (SDR; PreSens, Germany) optical oxygen sensing system (Soares et al. 2018). Before incubation start, the sensor vials were top-filled with sample water in a 20°C temperature controlled room and left for two hours with the cap open to equilibrate with the oxygen concentration in the air. The vials were then sealed without headspace or bubbles, inserted into the SDR plates and a first reading was carried out immediately to obtain a 100% DO calibration point. Thus all experiments started with nearly 100% DO saturation at 20°C (8.76 mg L^{-1}), before oxygen was gradually consumed during 28-d incubation in a closed PU-3J high precision temperature chamber (ESPEC, Japan). We used factory calibration data for the 0% DO calibration point, which is stable over time. The dissolved O_2 concentrations decreased in all incubations, but since this loss rate declined gradually over the course of the incubation, the oxygen (> 5.7 mg O_2 L^{-1}) was not exhausted in any of the cases.

187

188 In parallel, the remaining water in the 250 ml Nalgene bottles was incubated in a 20°C
189 constant room for the measurement of BP, absorbance and fluorescence during the
190 incubation. The BP was measured in a total of five 5 tubes per lake (day 1, 3, 7, 14 and 28)
191 using the 3H-leucine incorporation method (Smith and Azam 1992). Aliquots of 1.2 ml were
192 exposed to 40 nM leucine during 1 h, before the incubation was stopped with trichloroacetic
193 acid and the protein content was purified through repeated (three times) centrifugation and
194 removal of supernatant (Karlsson et al. 2001). Uptake of leucine was converted into bacterial
195 carbon (Simon and Azam 1989) applying the standard conversion factor 1.55 kg C mol leu^{-1}
196 multiplied with an isotopic dilution factor of 2. Total cumulative BP during the incubation
197 was calculated using the trapezoid rule.

198

199 *Reactivity continuum modeling*

200 The DOC decay was assessed using the reactivity continuum model (Boudreau and Ruddick
201 1991; Koehler et al. 2012), where the DOC concentration at time 't' relative to the initial
202 DOC concentration at time '0' (theoretical range from 0 to 1) was described as a function of
203 the rate parameter 'a' and the shape parameter 'υ' (Eq 1).

204 $$\frac{DOC_t}{DOC_0} = \left(\frac{a}{a+t}\right)^{\upsilon} \quad (1)$$

205 The model was fitted with days as time unit using the nonlinear least squares (nls) function in
206 R build 3.4.1 (R Development Core Team 2013). The accuracy of the model was given by the
207 root square mean error (RMSE) for deviations between predicted and measured relative DOC
208 concentrations. The apparent decay coefficients k for any time point was calculated (Eq 2).

209 $$k = \upsilon*(a + t)^{-1} \quad (2)$$

210

211 *Optical organic matter characterization*

Absorbance and excitation−emission matrices (EEMs) were collected at the beginning and at the end of the decay experiment using an Aqualog (Horiba Scientific). Scans were collected in a 1 cm quartz cuvette (2 s integration time) over 5 nm increments with excitation wavelengths ranging from 230 to 800 nm and emission wavelengths from 250 to 800 nm. The EEMs were blank-subtracted (Milli-Q water) daily, corrected for instrument-specific biases (Cory et al. 2010) and inner filter effects (Kothawala et al. 2013), and normalized to the Raman area of deionized (Milli-Q) water (Lawaetz and Stedmon 2009). Fluorescent components were identified with parallel factor analysis (PARAFAC) of the corrected EEMs using the toolbox and procedure described in Murphy et al. (2013). The PARAFAC model was validated using a split-half validation routine, core consistency diagnostic, and a visual inspection of the residuals to ensure no systematic signal remained (Fig. S3). Six fluorescent components were identified by the PARAFAC analysis: C1 and C3 (visible humic-like components; ex/em: 325/456 and 265-390/512 nm, respectively), C2 and C5 (UV humic-like components; ex/em: <250/446 nm and 255/438 nm, respectively), C4 (microbial humic-like component; ex/em: <250-305/406 nm), and C6 (tryptophan-like component; ex/em: 280/326 nm). All components have been previously listed in the online spectral library OpenFluor [www.openfluor.org; (Murphy et al. 2014)], and our model's emission and excitation loadings are available on the OpenFluor web site under the name "Swedish subarctic lakes" from the time of acceptance of this publication. These components are also shown visually in Fig. S3.

Colored dissolved organic matter (CDOM) was calculated as the absorbance at 440 nm, corrected for turbidity by subtracting the absorbance at 690 nm, and converted to Naperian units through division by cuvette length in meters and by multiplying with a correction factor of 2.303 (i.e. ln(10) which converts a decadic coefficient into a Naperian).

We chose not to include $SUVA_{254}$ and spectral slope in the analysis and presentation, because we did not have access to iron data and thus could not correct these parameters for potential iron interference which is particularly high in the ultraviolet region (Weishaar et al. 2003). As an alternative to $SUVA_{254}$, we used the ratio between CDOM at 440 mm (where iron interference is relatively lower) and DOC as a corresponding indicator. For reference, the ambient $SUVA_{254}$ in the selected study sites was 3.57 ± 0.77 (mean ± SD). Our analysis thus strongly focus on PARAFAC components, which have been shown to be little effected by iron, while maximizing the extracted information about DOM composition (Poulin et al. 2014). Moreover, we excluded several commonly reported standard spectral indices (Gabor et al. 2014), including the fluorescence index FI, humification index HIX, biological index BIX and the freshness index FRESH, because the change in these indices from the beginning to the end of our experiment was negligible (1-5% on average), and thus they were not informative about the major changes in DOM quality that occurred in response to the microbial processing of the DOM.

Element analyses

Dissolved organic carbon was measured via high temperature catalytic oxidation on a Shimadzu TOC-LCPH analyzer. The DOC concentrations are reported as the mean of three replicate injections for which the coefficient of variation was < 2%. The TP and TN were determined using a QuAAtro39 Continuous Segmented Flow Analyzer (SEAL Analytical), equipped with an auto sampler and ADM-unit (Autoclave Distillation Module). Samples were processed through two-stage on-line digestion with potassium persulfate at 110°C, first under alkaline conditions and then under acidic conditions, both under a pressure of 0.09 MPa. The TN was analyzed as nitrite under chemical reactions to form an azo dye measured

262 at 550 nm, while TP was analyzed through a colored reaction by molybdenum blue and
263 measured at 880 nm.

264 RESULTS

265 The mean O_2-inferred DOC decreased by 20% during the 28 days of incubation. In spite of
266 the storage time prior to the experiment, there was surprisingly good preservation of the most
267 labile DOC fraction, evident from the distinct high decay rates found during the first days of
268 the bio-decay experiment (Fig. 1). Based on the observed dissolved oxygen changes during
269 incubation (Fig. 1a) and the known initial DOC concentrations, the fraction DOC remaining
270 over time could be calculated and used to fit the reactivity continuum model, yielding low
271 average RMSE values (0.45%) in the range of 0.06-2.8%. The modeled estimates of the
272 apparent decay coefficient k spanned from 0.006 to 0.092 at t = 0 days and from 0.001 to
273 0.017 at t = 28 days (Fig. 1b). The bacterial production showed a similar pattern of highly
274 variable values between sites, and a slightly decreasing trend over time (Fig. 1c). The total
275 bacterial production during the incubation period amounted to 0.2-11.5% of the initial DOC,
276 with a mean of 3.6%.

277

278 While the average DOC decreased (paired $t < -76.3$), from 3.5 mg L^{-1} initially to 2.8 mg L^{-1} at
279 the end of the experiment, CDOM and FDOM increased from 1.7 m^{-1} to 2.0 m^{-1} (paired $t >$
280 10.7) and from 4.5 R.U. to 5.9 R.U (paired $t > 28.4$), respectively (2-tail $p < 0.001$, $n = 101$;
281 see standard deviation of means in Fig. 2a). As a consequence, the ratio between CDOM and
282 DOC increased 1.7 times and the ratio between FDOM and DOC increased 1.8 times (Fig.
283 2a). Among the six components of FDOM identified using PARAFAC (see description in
284 methods), all were produced (1-sample $t > 9.1$) except for one of the humic-like components
285 (C2) which was net consumed (1-sample $t < -21.4$, 2-tail $p < 0.001$, $n = 101$; Fig. 2b). The
286 components showing the largest production rates were the protein-like component C6 (mean
287 0.007 R.U. d^{-1}) and, especially, the humic-like component C5 (mean 0.048 R.U. d^{-1}).

288

289 Bacterial production rates at the end of the incubation showed weak positive correlations with
290 TN and TP (Table S1), but there were no clear indications of nutrient limitation in the DO
291 consumption experiments used to model the DOC decay. On the contrary, initial and final
292 decay coefficients as well as the total DOC loss were negatively correlated to nutrient
293 concentrations. Among the site characteristics, lake area, elevation and longitude showed
294 relatively few and weak correlations with decay variables. However, decay (k) coefficients,
295 total DOC loss and carbon use for bacterial production correlated positively with latitude and
296 negatively with CDOM and FDOM (Table S1).
297
298 In general, relative (%) abundances of the fluorescence components classically interpreted as
299 terrestrially-derived humic (C1-C3) were negatively related to different aspects of DOC
300 reactivity and use by bacteria, while the microbially derived humic C4, the humic-like C5,
301 and the protein-like (C6) components were positively related to these decay variables (Table
302 S2). Component C6 was the strongest positive indicator of both total DOC loss (Pearson r =
303 0.56, r^2 = 0.32, n = 101, $p < 0.001$; Fig. 3a) and total share of DOC used for bacterial
304 production (Pearson r = 0.55, r^2 = 0.31, n = 101, $p < 0.001$; Fig. 3b). The corresponding
305 relationships for components C1, C2 and C3 had similar strengths, but these correlations
306 were negative (Table S2).
307
308 Although most lakes of the study area can be characterized as clear-water oligotrophic, there
309 was a 27-fold variability in ambient CDOM, with a few values spanning up toward 8 m^{-1}. The
310 patterns of change in concentration and optical properties of DOC that we observed during
311 the incubation experiment were not randomly distributed along this gradient of increasing
312 CDOM. For example, the rate of change in the humic-like C2 (R.U. d^{-1}) followed a
313 logarithmic function of CDOM m^{-1} (y = -0.0066*ln(x) + 0.014, R^2 = 0.30, n = 101, $p < 0.001$;

Fig. 4a) implying that more of C2 was consumed with increasing brownness of the water, but in contrast the combined change in C1, C3, and C5 followed a logarithmic curve that increased along the CDOM gradient ($y = 0.0094*\ln(x) + 0.051$, $R^2 = 0.16$, $n = 101$, $p < 0.001$; Fig. 4a). Production rates of the microbial-like component C4 were unrelated to the CDOM gradient. Noteworthy, production of protein-like fluorescence (C6) was characteristic of lakes with low ambient CDOM, and C6 production rates decreased with the CDOM gradient toward zero in the brownest lakes ($y = -0.0029*\ln(x) + 0.0082$, $R^2 = 0.20$, $n = 101$, $p < 0.001$; Fig. 4a). Moreover the reactivity of the DOC (initial k) decreased as a power function of increasing *in situ* CDOM ($0.024*x^{-0.372}$, $R^2 = 0.25$, $n = 101$, $p < 0.001$; Fig. 4c).

The pattern of accumulating protein-like fluorescence together with strongly decreasing k during the degradation experiments created a paradoxical negative relationship between k and protein-like fluorescence in absolute units in all of the data combined (Fig. 5). This reverse relationship was enhanced by the fact that C6 occurred in high absolute concentrations (but low relative concentrations) in some of the browner lakes that were also characterized by low k values. Thus, although the relative (%) abundance of C6 was a strong positive indicator of different aspects of DOC reactivity (Fig. 3), the relationship between k and C6 in absolute units surprisingly was negative (Fig. 5).

333 DISCUSSION

334 Our survey of subarctic lakes confirms the existing knowledge on how increased CDOM in
335 freshwaters is associated to changes in the composition and biological reactivity of DOM
336 (Fasching et al. 2014; Hopkinson et al. 1998; Koehler et al. 2012). However, for the first time
337 we also show that in these subarctic lakes there is a systematic microbial production of
338 CDOM and FDOM that, in turn, shows patterns across the gradient of ambient water
339 brownness. Thus, browning of subarctic tundra lakes may not only affect the concentration,
340 composition and reactivity of DOM, but it also impacts on interactions between bacteria and
341 DOM that further modifies the pool of optically active DOM. Hence, our laboratory results
342 suggest a previously unrecognized feedback mechanism of relevance for assessing the
343 changes in subarctic lakes due to climate-induced increases in CDOM loading from the
344 catchment. However, further research is needed to validate the representativeness of these
345 laboratory results to field conditions.
346
347 There was an expected pattern of decreasing initial k values with increasing CDOM (Fig. 4c),
348 in parallel with decreasing percentage protein-like fluorescence. These results agree with the
349 pattern that Koehler et al. (2012) found in a comparison between clear-water and brown-
350 water boreal lakes, caused by a decreasing share of labile algal DOM with increasing CDOM.
351 In our study we did not investigate the origin of the DOM in the lakes, but previous studies
352 have shown that low CDOM values combined with large fractions of protein-like
353 fluorescence are indicative of major algal contributions to the DOM pool (Guillemette and
354 del Giorgio 2011; Stedmon and Markager 2005) which could explain the high k values and
355 large proportion of DOC used for bacterial production in lakes with low CDOM (Table S1)
356 and high percentage protein-like fluorescence (Fig. 3). Interestingly, in terms of the absolute
357 (mg L^{-1}) DOC decay, the decreasing k values along the CDOM gradient were compensated

by increasing DOC concentrations, such that there was no correlation between the total absolute DOC loss (final minus initial values in mg L^{-1}) and increasing CDOM (p = 0.86, not shown). Thus, contrary to what Lapierre et al. (2013) found for boreal lakes, increased CDOM in our study does not appear to imply that the total concentration of labile carbon increases in the water column of lakes, at least not during the autumn (and low discharge) conditions when our measurements were performed. However, during other seasons such as the snowmelt season (spring-midsummer) when fresh colored terrestrial DOC is entering the lakes, previous studies in our study area indicate the respiration is boosted also in absolute carbon units, leading to substantial CO_2 emissions (Jonsson et al. 2007; Jonsson et al. 2003).

Our initial apparent k values were considerably higher than those found in other lake studies using 20°C dark incubations (Koehler et al. 2012; Mostovaya et al. 2016). A possible reason for this difference is that the previous studies measured DOC concentrations with low temporal resolution (several days per measurement) while we used a high temporal resolution optical sensor approach, allowing us to detect some of the most labile DOC fractions used in the very beginning of the decay (Guillemette and del Giorgio 2011; Pollard 2013). After a few days of incubation, our k values had decreased to a range that represent the reactivity of a wide range of typical DOC molecules found in lakes (Mostovaya et al. 2017), which together with low RMSE gives credibility to the modeled DOC decay.

Due to logistic challenges with measuring the DOC decay directly in a large number of samples, we were limited to indirect DOC assessment based on an oxygen sensing system. A weakness with this approach is the uncertainty related to the RQ value used for unit conversion to carbon. Studies in unproductive lakes in different boreal regions have reported average bacterioplankton RQs of 1.2 (Berggren et al. 2012) or ~2 (Cimbleris and Kalff 1998),

383 and RQs as high as ~3 have been experimentally achieved by feeding bacteria with UV light
384 treated partially oxidized DOC (Allesson et al. 2016). Considering that partial UV oxidation
385 followed by microbial decay could be a major pathway of organic carbon decay in tundra
386 region freshwaters (Cory et al. 2014), it is possible that the RQ and thus also the DOC decay
387 rates in this study were underestimated. However, this should be particularly true for the
388 clearest and thus most UV light exposed lakes, which would further amplify the pattern of
389 high k values in lakes with low CDOM (Fig. 4c). Therefore, if the RQ value biased our
390 results it would not necessarily mean that any conclusion from the study is wrong, but rather
391 that the strength in some of the reported patterns might be underestimated.
392
393 We found support for the hypothesis that bulk FDOM and its sub-components (except C2)
394 are net produced in clear-water subarctic tundra lakes, as expected due to low terrestrial
395 influence relative to that of algal derived DOM, which can lead to FDOM production within
396 the lakes (Fox et al. 2017). This agrees with the temperate lake study by Guillemette and del
397 Giorgio (2012), where both protein- and humic-like FDOM were microbially net produced in
398 clear lakes (CDOM < 2) that had significant algal DOM fractions. However, while their study
399 suggested a generic shift to net FDOM production at a certain level of terrestrial influence
400 (CDOM > 2, terrigenous DOM > ~85%) (Guillemette and del Giorgio 2012), we did not
401 reach a corresponding threshold that shifted the production-consumption balances of all
402 FDOM components, but instead there were variable responses among the FDOM components
403 to the increasing CDOM (Fig. 4). In our case, the protein-like fluorescence was produced the
404 most in the clearest lakes, but even if the production decreased with increasing CDOM the
405 values remained positive throughout the color gradient Fig. 4b. The humic-like components,
406 on the other hand, were in our study processed to a larger degree with higher CDOM, either
407 through increased production (C1, C3 and C5) or increased consumption (C2). Thus the

408 microbial-induced dynamics of FDOM appear to be remarkably different in subarctic lakes
409 compared to boreal and temperate lakes (Guillemette and del Giorgio 2012).
410
411 Our study demonstrates counter-intuitive aspects of protein-like fluorescence dynamics in
412 lakes. First, while the relative C6 *in situ* abundance (%) in the study lakes was negatively
413 correlated to CDOM, there was an increase in the absolute (R.U.) C6 concentration along the
414 CDOM gradient because of the associated increases in total FDOM (Table S2). This reflects
415 that protein-like FDOM may arrive in high absolute (but low relative) concentrations with
416 terrestrial drainage water (Lapierre and del Giorgio 2014). Second, our incubations showed
417 that C6 was produced in parallel with microbial consumption of labile DOC, but the protein-
418 like FDOM itself was not very reactive as it tended to accumulate during the incubations.
419 These two aspects together shaped an unexpected reversed (negative) relationship between
420 reactivity (k) and the absolute concentration of protein-like fluorescence (Fig. 5), adding to
421 the emerging view that predictions of reactivity based on FDOM must be made with great
422 caution because the relationships are indirect and their causality is not straightforward (Fox et
423 al. 2017). Our findings also help explain why protein-like DOM appears as persistent
424 (refractory) in nature along spatial gradients of increasing water residence times (Kellerman
425 et al. 2015) or over time in slow-turnover lakes (Goldberg et al. 2015).
426
427 Another surprising result was that not only FDOM, but also CDOM, increased systematically
428 in our incubation experiments (Fig. 1). Such observations of increasing CDOM in dark
429 bacterial incubations have only rarely been observed before (Berggren et al. 2018). However,
430 it has been long known that bacterioplankton can excrete or by other means produce CDOM
431 (Shimotori et al. 2009; Tranvik 1993), at the same time as they tend to prefer consuming non-
432 colored DOM fractions (Asmala et al. 2014; Berggren et al. 2018; Hansen et al. 2016).

433 Theoretically, this makes it possible for bacteria to make a net contribution to CDOM,
434 especially in lakes where non-colored algal DOC may be a main carbon source. However,
435 whether or not this CDOM production alongside with FDOM production that we observed is
436 representative to *in situ* conditions can merely be speculated on, given the artificial dark
437 environment in our experiment and the preceding 40-d refrigerated sample storage time that
438 likely altered the composition of the microbial community (Calvo-Diaz et al. 2011).
439 Nonetheless, if assuming representativeness, then the measured bulk CDOM and FDOM
440 production would be sufficient for renewing the ambient respective pools in 104 d and 82 d,
441 respectively (median for all lakes) under steady-state conditions. This highlights the need to
442 perform further research on the origin of optically active compounds in lakes, as the
443 commonly assumed terrestrial origin of colored DOM constituents in lakes may not always
444 be true.
445
446 The average CDOM production (0.37 m^{-1} in total during 28 d) was evenly distributed across
447 the CDOM gradient (0.29-7.8 m^{-1}), but its relative importance was largest in the clearest
448 lakes. In fact, the measured microbial CDOM and FDOM production rates would be
449 theoretically sufficient (again, assuming steady-state conditions and data representativeness)
450 to renew the bulk CDOM and FDOM pools in a many of the clearest lakes during e.g. a 2-
451 month summer period with stagnant water. In lakes with long water residence times (a few
452 years) it could be hypothesized that the internal production of CDOM and FDOM is always
453 larger than the input of these components from the catchment. Thus, in such lakes it can be
454 expected that CDOM is mainly controlled by the balance between microbial CDOM
455 production and photochemical CDOM removal by sunlight (Cory et al. 2014).
456

In summary, this study shows that clear-water subarctic lakes in northern Sweden had high DOC reactivity (high k values), high bacterial production per unit DOC, and FDOM production characterized by increases in protein-like fluorescence. Relatively browner lakes had lower k values and relatively less production of biomass and protein-like fluorescence. Our study is the first to suggest that DOM in subarctic clear waters may derive its characteristically high protein-like fluorescence from internal microbial production, but this effect appears to be limited to lakes with low CDOM. Thus, water 'browning' can be expected to impact the internal processes that control the balance between renewal and turnover of optically active organic matter in the water, potentially with fundamental consequences for the functioning of these ecosystems.

467 REFERENCES

468 Åkerman, H. J., and M. Johansson. 2008. Thawing permafrost and thicker active layers in sub-arctic
469 Sweden. Permafrost Periglacial Process. **19:** 279-292.
470 Allesson, L., L. Ström, and M. Berggren. 2016. Impact of photochemical processing of DOC on the
471 bacterioplankton respiratory quotient in aquatic ecosystems. Geophysical Research Letters
472 **43:** 7538-7545.
473 Asmala, E., R. Autio, H. Kaartokallio, C. A. Stedmon, and D. N. Thomas. 2014. Processing of humic-
474 rich riverine dissolved organic matter by estuarine bacteria: effects of predegradation and
475 inorganic nutrients. Aquatic Sciences **76:** 451-463.
476 Berggren, M. and others 2018. Quality transformation of dissolved organic carbon during water
477 transit through lakes: contrasting controls by photochemical and biological processes.
478 Biogeosciences **15:** 457-470.
479 Berggren, M., J. F. Lapierre, and P. A. Del Giorgio. 2012. Magnitude and regulation of
480 bacterioplankton respiratory quotient across freshwater environmental gradients. Isme J. **6:**
481 984-993.
482 Berggren, M., R. A. Sponseller, A. R. Alves Soares, and A. K. Bergström. 2015. Toward an
483 ecologically meaningful view of resource stoichiometry in DOM-dominated aquatic systems.
484 Journal of Plankton Research **37:** 489-499.
485 Berggren, M. and others 2010. Lake secondary production fueled by rapid transfer of low molecular
486 weight organic carbon from terrestrial sources to aquatic consumers. Ecology Letters **13:** 870-
487 880.
488 Boudreau, B. P., and B. R. Ruddick. 1991. On a reactive continuum representation of organic matter
489 diagenesis. Am. J. Sci. **291:** 507-538.
490 Brown, J., O. J. Ferrians Jr, J. A. Heginbottom, and E. S. Melnikov. 1997. Circum-arctic map of
491 permafrost and ground-ice conditions. USGS Circum-pacific map.
492 Callaghan, T. V., B. R. Werkman, and R. M. M. Crawford. 2002. The tundra-taiga interface and its
493 dynamics: Concepts and applications. Ambio **Special Report Number 12:** 6-14.

494 Calvo-Diaz, A., L. Diaz-Perez, L. A. Suarez, X. A. G. Moran, E. Teira, and E. Maranon. 2011.
495 Decrease in the autotrophic-to-heterotrophic biomass ratio of picoplankton in oligotrophic
496 marine waters due to bottle enclosure. Applied and Environmental Microbiology **77:** 5739-
497 5746.
498 Cimbleris, A. C. P., and J. Kalff. 1998. Planktonic bacterial respiration as a function of C : N : P ratios
499 across temperate lakes. Hydrobiologia **384:** 89-100.
500 Cory, R. M., M. P. Miller, D. M. McKnight, J. J. Guerard, and P. L. Miller. 2010. Effect of
501 instrument-specific response on the analysis of fulvic acid fluorescence spectra. Limnology
502 and Oceanography-Methods **8:** 67-78.
503 Cory, R. M., C. P. Ward, B. C. Crump, and G. W. Kling. 2014. Sunlight controls water column
504 processing of carbon in arctic fresh waters. Science **345:** 925-928.
505 Creed, I. F. and others 2018. Global change-driven effects on dissolved organic matter composition:
506 Implications for food webs of northern lakes. Global Change Biology **24:** 3692-3714.
507 Fasching, C., B. Behounek, G. A. Singer, and T. J. Battin. 2014. Microbial degradation of terrigenous
508 dissolved organic matter and potential consequences for carbon cycling in brown-water
509 streams. Sci Rep **4:** 4981.
510 Fox, B. G., R. M. S. Thorn, A. M. Anesio, and D. M. Reynolds. 2017. The in situ bacterial production
511 of fluorescent organic matter; an investigation at a species level. Water Research **125:** 350-
512 359.
513 Gabor, R. S., A. Baker, D. M. McKnight, and M. P. Miller. 2014. Fluorescence indices and their
514 interpretation, p. 303-338. *In* A. Baker, D. M. Reynolds, J. Lead, P. G. Coble and R. G. M.
515 Spencer [eds.], Aquatic organic matter fluorescence. Cambridge Environmental Chemistry
516 Series. Cambridge University Press.
517 Gisnås, K. and others 2017. Permafrost map for Norway, Sweden and Finland. Permafrost Periglacial
518 Process. **28:** 359-378.
519 Goldberg, S. J. and others 2015. Refractory dissolved organic nitrogen accumulation in high-elevation
520 lakes. Nat. Commun. **6**.

521 Guillemette, F., and P. A. del Giorgio. 2011. Reconstructing the various facets of dissolved organic
522 carbon bioavailability in freshwater ecosystems. Limnology and Oceanography **56:** 734-748.
523 ---. 2012. Simultaneous consumption and production of fluorescent dissolved organic matter by lake
524 bacterioplankton. Environ. Microbiol. **14:** 1432-1443.
525 Hansen, A. M., T. E. C. Kraus, B. A. Pellerin, J. A. Fleck, B. D. Downing, and B. A. Bergamaschi.
526 2016. Optical properties of dissolved organic matter (DOM): Effects of biological and
527 photolytic degradation. Limnology and Oceanography **61:** 1015-1032.
528 Hijmans, R. J., S. E. Cameron, J. L. Parra, P. G. Jones, and A. Jarvis. 2005. Very high resolution
529 interpolated climate surfaces for global land areas. Int J Climatol **25:** 1965-1978.
530 Hopkinson, C. S. and others 1998. Terrestrial inputs of organic matter to coastal ecosystems: An
531 intercomparison of chemical characteristics and bioavailability. Biogeochemistry **43:** 211-
532 234.
533 Jansson, M., P. Ask, J. Ask, P. Bystrom, J. Karlsson, and L. Persson. 2010. Climate impacts on high
534 latitude lakes, p. 80-81. *In* J. Settele et al. [eds.], Atlas of biodiversity risk. Pensoft.
535 Jansson, M., L. Persson, A. M. DeRoos, R. I. Jones, and L. J. Tranvik. 2007. Terrestrial carbon and
536 intraspecific size-variation shape lake ecosystems. Trends in Ecology & Evolution **22:** 316-
537 322.
538 Jennings, M., H. Abdulla, A. Stubbins, L. Sun, R. Wang, and K. Mopper. 2018. A dissolved organic
539 carbon (DOC) analyzer capable of detecting sub-mu M DOC differences in natural fresh
540 waters: A proof of concept study. Limnology and Oceanography-Methods **16:** 309-321.
541 Jonsson, A., J. Aberg, and M. Jansson. 2007. Variations in pCO(2) during summer in the surface
542 water of an unproductive lake in northern Sweden. Tellus Series B-Chemical and Physical
543 Meteorology **59:** 797-803.
544 Jonsson, A., J. Karlsson, and M. Jansson. 2003. Sources of carbon dioxide supersaturation in
545 clearwater and humic lakes in northern Sweden. Ecosystems **6:** 224-235.
546 Karlsson, J., P. Byström, J. Ask, P. Ask, L. Persson, and M. Jansson. 2009. Light limitation of
547 nutrient-poor lake ecosystems. Nature **460:** 506-509.

548 Karlsson, J., A. Jonsson, and M. Jansson. 2001. Bacterioplankton production in lakes along an altitude
549 gradient in the subarctic north of Sweden. Microbial Ecology **42:** 372-382.
550 Kellerman, A. M., D. N. Kothawala, T. Dittmar, and L. J. Tranvik. 2015. Persistence of dissolved
551 organic matter in lakes related to its molecular characteristics. Nat. Geosci. **8:** 454-U452.
552 Koehler, B., E. von Wachenfeldt, D. Kothawala, and L. J. Tranvik. 2012. Reactivity continuum of
553 dissolved organic carbon decomposition in lake water. Journal of Geophysical Research-
554 Biogeosciences **117:** G01024.
555 Kothawala, D. N., K. R. Murphy, C. A. Stedmon, G. A. Weyhenmeyer, and L. J. Tranvik. 2013. Inner
556 filter correction of dissolved organic matter fluorescence. Limnology and Oceanography-
557 Methods **11:** 616-630.
558 Kullman, L. 2002. Rapid recent range-margin rise of tree and shrub species in the Swedish Scandes. J.
559 Ecol. **90:** 68-77.
560 ---. 2014. Treeline (Pinus sylvestris) landscape evolution in the Swedish Scandes - a 40-year
561 demographic effort viewed in a broader temporal context. Norsk Geogr Tidsskr **68:** 155-167.
562 Lapierre, J. F., and P. A. del Giorgio. 2014. Partial coupling and differential regulation of biologically
563 and photochemically labile dissolved organic carbon across boreal aquatic networks.
564 Biogeosciences **11:** 5969-5985.
565 Lapierre, J. F., F. Guillemette, M. Berggren, and P. A. del Giorgio. 2013. Increases in terrestrially
566 derived carbon stimulate organic carbon processing and CO2 emissions in boreal aquatic
567 ecosystems. Nat. Commun. **4:** 2972.
568 Lawaetz, A. J., and C. A. Stedmon. 2009. Fluorescence intensity calibration using the raman scatter
569 peak of water. Appl Spectrosc **63:** 936-940.
570 Lawrence, D. M., A. G. Slater, and S. C. Swenson. 2012. Simulation of present-day and future
571 permafrost and seasonally frozen ground conditions in CCSM4. J. Clim. **25:** 2207-2225.
572 Miller, M. P., and D. M. McKnight. 2010. Comparison of seasonal changes in fluorescent dissolved
573 organic matter among aquatic lake and stream sites in the Green Lakes Valley. Journal of
574 Geophysical Research-Biogeosciences **115**.

575 Mostovaya, A., J. A. Hawkes, B. Koehler, T. Dittmar, and L. J. Tranvik. 2017. Emergence of the
576 reactivity continuum of organic matter from kinetics of a multitude of individual molecular
577 constituents. Environmental Science & Technology **51:** 11571-11579.
578 Mostovaya, A., B. Koehler, F. Guillemette, A. K. Brunberg, and L. J. Tranvik. 2016. Effects of
579 compositional changes on reactivity continuum and decomposition kinetics of lake dissolved
580 organic matter. Journal of Geophysical Research-Biogeosciences **121:** 1733-1746.
581 Murphy, K. R., C. A. Stedmon, D. Graeber, and R. Bro. 2013. Fluorescence spectroscopy and multi-
582 way techniques. PARAFAC. Anal Methods-Uk **5:** 6557-6566.
583 Murphy, K. R., C. A. Stedmon, P. Wenig, and R. Bro. 2014. OpenFluor- an online spectral library of
584 auto-fluorescence by organic compounds in the environment. Anal Methods-Uk **6:** 658-661.
585 Nayar, S., and L. M. Chou. 2003. Relative efficiencies of different filters in retaining phytoplankton
586 for pigment and productivity studies. Estuarine Coastal and Shelf Science **58:** 241-248.
587 Pollard, P. C. 2013. In situ rapid measures of total respiration rate capture the super labile DOC
588 bacterial substrates of freshwater. Limnology and Oceanography-Methods **11:** 584-593.
589 Poulin, B. A., J. N. Ryan, and G. R. Aiken. 2014. Effects of iron on optical properties of dissolved
590 organic matter. Environmental Science & Technology **48:** 10098-10106.
591 R Development Core Team. 2013. R: A language and environment for statistical computing.
592 Romera-Castillo, C., H. Sarmento, X. A. Alvarez-Salgado, J. M. Gasol, and C. Marrase. 2011. Net
593 production and consumption of fluorescent colored dissolved organic matter by natural
594 bacterial assemblages growing on marine phytoplankton exudates. Applied and
595 Environmental Microbiology **77:** 7490-7498.
596 Rowe, O. F., J. Dinasquet, J. Paczkowska, D. Figueroa, L. Riemann, and A. Andersson. 2018. Major
597 differences in dissolved organic matter characteristics and bacterial processing over an
598 extensive brackish water gradient, the Baltic Sea. Marine Chemistry **202:** 27-36.
599 Shimotori, K., Y. Omori, and T. Hama. 2009. Bacterial production of marine humic-like fluorescent
600 dissolved organic matter and its biogeochemical importance. Aquatic Microbial Ecology **58:**
601 55-66.

602 Simon, M., and F. Azam. 1989. Protein content and protein synthesis rates of planktonic marine
603 bacteria. Marine Ecology-Progress Series **51:** 201-213.
604 Smith, D. C., and F. Azam. 1992. A simple, economical method for measuring bacterial protein
605 synthesis rates in seawater using 3H-leucine. Marine Microbial Food Webs **6:** 107-114.
606 Soares, A. R. A., E. S. Kritzberg, I. Custelcean, and M. Berggren. 2018. Bacterioplankton responses
607 to increased organic carbon and nutrient loading in a boreal estuary-separate and interactive
608 effects on growth and respiration. Microbial Ecology **76:** 144-155.
609 Solomon, C. T. and others 2015. Ecosystem consequences of changing inputs of terrestrial dissolved
610 organic matter to lakes: current knowledge and future challenges. Ecosystems **18:** 376-389.
611 Stedmon, C. A., and S. Markager. 2005. Tracing the production and degradation of autochthonous
612 fractions of dissolved organic matter by fluorescence analysis. Limnology and Oceanography
613 **50:** 1415-1426.
614 Tranvik, L. J. 1993. Microbial transformation of labile dissolved organic-matter into humic-like
615 matter in seawater. FEMS Microbiology Ecology **12:** 177-183.
616 Urtizberea, A., N. Dupont, R. Rosland, and D. L. Aksnes. 2013. Sensitivity of euphotic zone
617 properties to CDOM variations in marine ecosystem models. Ecol. Model. **256:** 16-22.
618 Vincent, W. F., I. Laurion, R. Pienitz, and K. M. Walter. 2012. Climate impacts on arctic lake
619 ecosystems, p. 27-42. *In* C. R. Goldman, M. Kumagai and R. D. Robarts [eds.], Climatic
620 change and global warming of inland waters: impacts and mitigation for ecosystems and
621 societies. John Wiley & Sons.
622 Virtanen, R. and others 2016. Where do the treeless tundra areas of northern highlands fit in the
623 global biome system: toward an ecologically natural subdivision of the tundra biome. Ecol
624 Evol **6:** 143-158.
625 Wauthy, M. and others 2018. Increasing dominance of terrigenous organic matter in circumpolar
626 freshwaters due to permafrost thaw. Limnology and Oceanography Letters **3:** 186-198.
627 Weishaar, J. L., G. R. Aiken, B. A. Bergamaschi, M. S. Fram, R. Fujii, and K. Mopper. 2003.
628 Evaluation of specific ultraviolet absorbance as an indicator of the chemical composition and
629 reactivity of dissolved organic carbon. Environmental Science & Technology **37:** 4702-4708.

630 Wetzel, R. G. 1995. Death, detritus, and energy flow in aquatic ecosystems. Freshwater Biology **33:**
631 83-89.
632 Wielgolaski, F. E. 2005. History and environment of the Nordic mountain birch, p. 3-18. *In* F. E.
633 Wielgolaski, P. S. Karlsson, S. Neuvonen and D. Thannheiser [eds.], Plant ecology,
634 herbivory, and human impact in Nordic mountain birch forests. Ecological Studies. Springer
635 Verlag.
636 Williamson, C. E. and others 2015. Ecological consequences of long-term browning in lakes. Sci Rep
637 **5:** 18666.

638

639 TABLES

640 Table 1. Ambient nutrient concentrations, geographical settings and optical characteristics of
641 101 subarctic Swedish lakes. Variables represent dissolved organic carbon (DOC), total
642 nitrogen (TN), total phosphorus (TP), lake area/location, colored dissolved organic matter at
643 440 nm wavelength (CDOM), total fluorescent dissolved organic matter (FDOM) and relative
644 contributions from the six different components of FDOM (C1-C6). The three respective data
645 columns show overall range, median (interquartile range in brackets) and mean (standard
646 deviation in brackets).

Variable	Range	Median [IQR]	Mean [SD]
DOC (mg L^{-1})	1.6-9.6	3.1 [2.5-4.2]	3.5 [1.6]
TN (mg L^{-1})	0.06-0.39	0.16 [0.11-0.20]	0.16 [0.06]
TP (µg L^{-1})	1.1-22.6	3.8 [2.8-5.9]	4.8 [3.4]
Area (ha)	0.1-112.8	1.0 [0.7-2.1]	3.2 [11.4]
Elevation (m a.s.l.)	326-587	444 [409-491]	447 [59]
Latitude (DD)	68.44-68.50	68.46 [68.45-68.48]	68.47 [0.02]
Longitude (DD)	18.19-18.65	18.43 [18.31-18.54]	18.43 [0.13]
CDOM (m^{-1})	0.3-7.8	1.3 [0.8-2.1]	1.7 [1.2]
FDOM (R.U.)	1.2-13.4	4.1 [3.1-5.8]	4.5 [2.1]
C1 (%)	13.9-24.9	19.7 [18.1-21]	19.6 [2.2]
C2 (%)	26.9-43.2	37.3 [35.1-38.4]	36.6 [2.7]
C3 (%)	7.9-14.0	11.1 [10.4-12.1]	11.2 [1.3]
C4 (%)	15.7-21.6	18.1 [17.3-18.9]	18.1 [1.2]
C5 (%)	0.0-5.4	2.3 [1.5-3.3]	2.3 [1.3]
C6 (%)	4.7-32.4	11.4 [8.9-14.7]	12.2 [4.6]

647

FIGURES

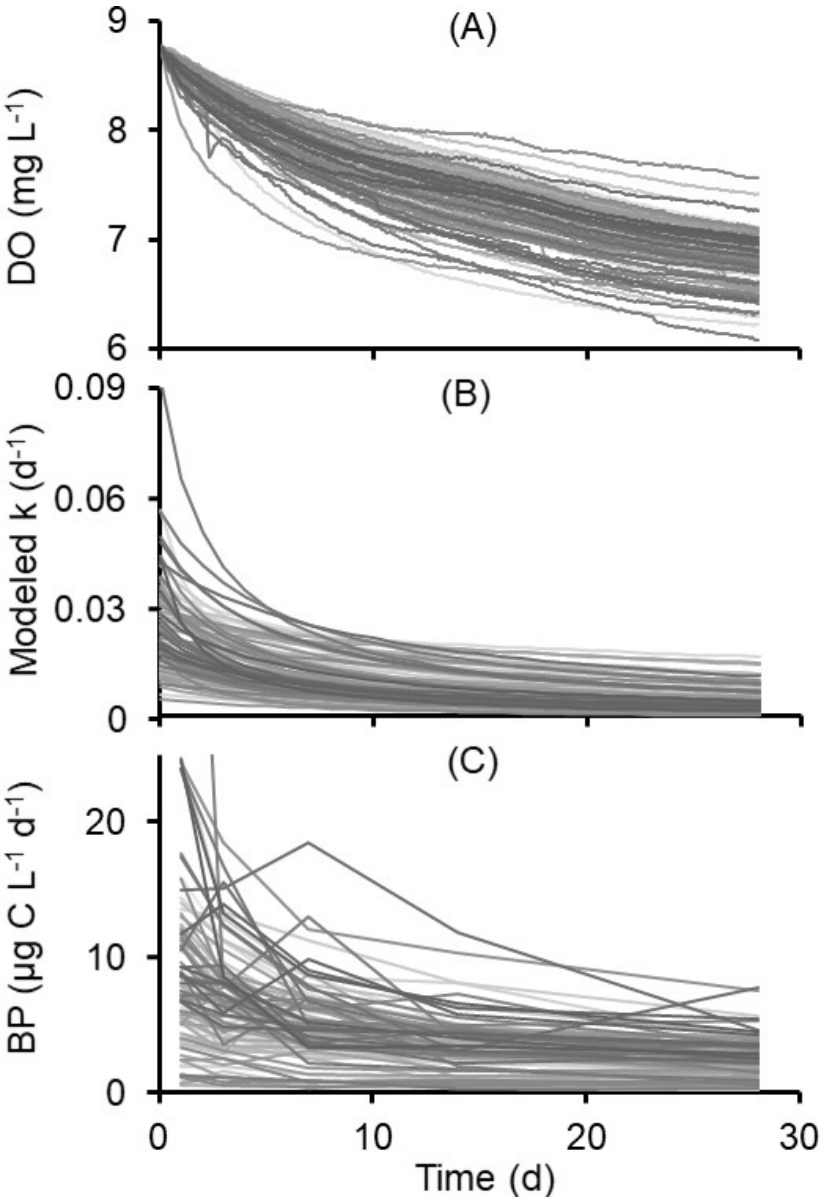

Figure 1. Visual presentation of the variability in in measured and models variables during 28-day dark incubations of water from 101 lakes in a Swedish tundra landscape. Charts show (A) observed dissolved oxygen, (B) decay coefficient k for the calculated (based on dissolved oxygen changes) degradation of dissolved organic carbon, and (C) measured bacterial production rates. The y axis of panel C is limited to 25 µg L^{-1}, which excludes one high BP value of 72 µg C L^{-1} at t = 1. The grey scale coloring of the curves (A-C) is random, to visually separate the lines.

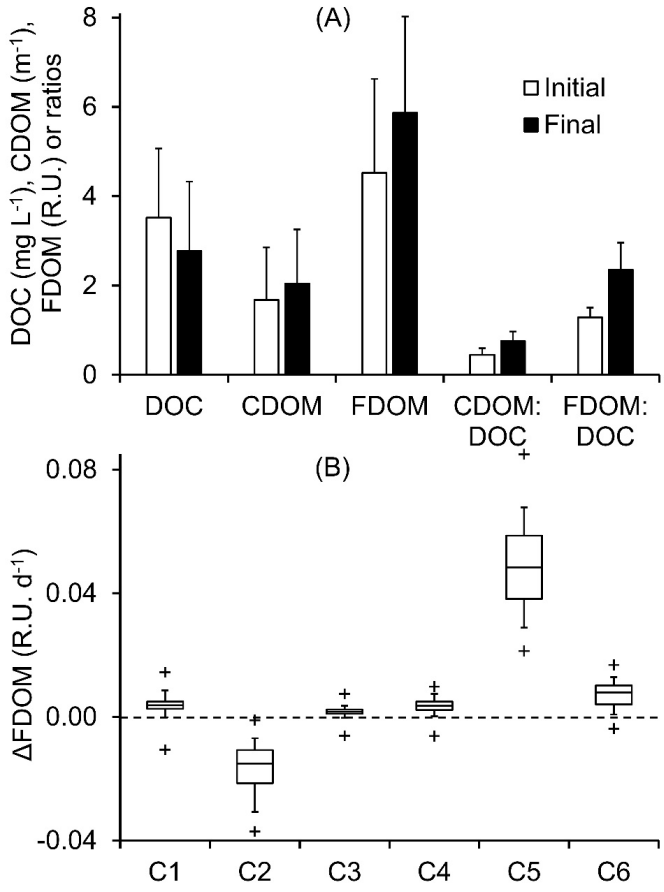

Figure 2. (A) Initial and final incubation values for dissolved organic carbon (DOC; measured initial values and final values inferred from dissolved oxygen change), colored dissolved organic matter (CDOM), fluorescent dissolved organic matter (FDOM), and ratios between these variables during 28-day dark laboratory incubations of water from 101 subarctic tundra lakes. Bars show mean values and error bars standard deviations. Note that while the overall distributions overlap for each variable, the paired differences between initial and final values for each respective variable are highly significant ($t > 10.7$ or $t < -76.3$ or, $n = 101$, 2-tail $p < 0.001$, paired t-test). (B) Box and whisker plots for production rates of six PARAFAC-derived subcomponents of FDOM during incubation. Boxes show quartiles two and three, lower and upper whiskers the 5th and 95th percentiles, respectively, and plus symbols minimum/maximum values. The mean Δ vales of all components are significantly different from zero ($t > 9.1$ or $t < -21.4$, $n = 101$, 2-tail $p < 0.001$, 1-sample t-test).

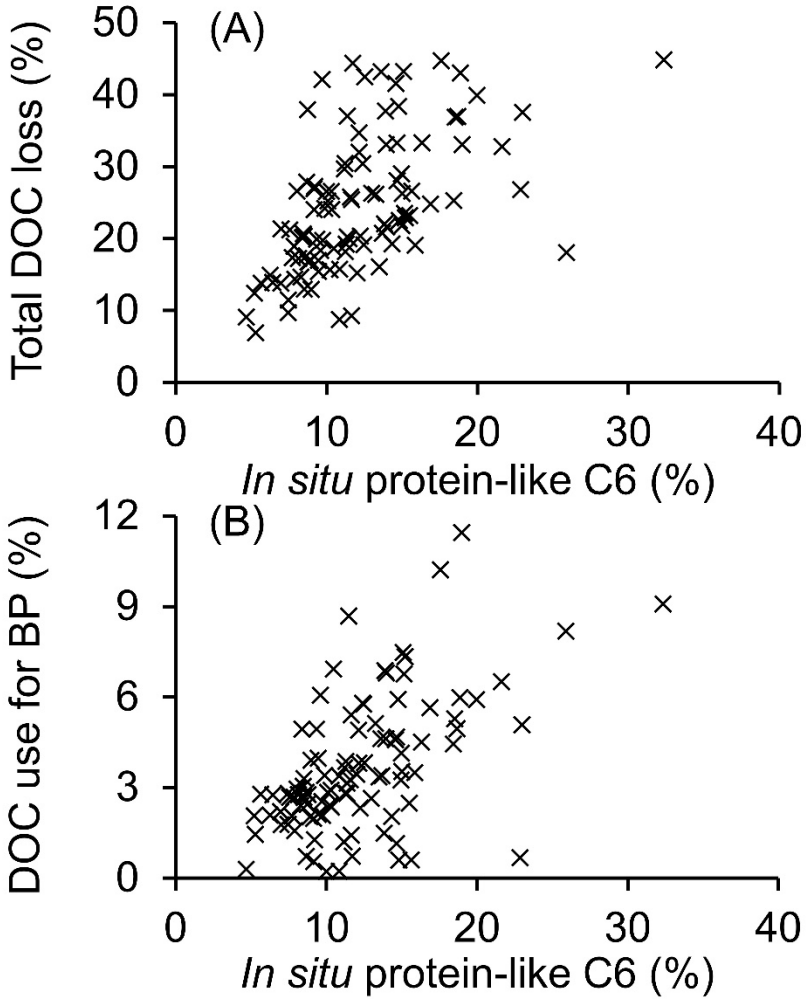

Figure 3. Microbial use of dissolved organic (DOC) during 28-d dark laboratory incubations of water from 101 lakes in a subarctic tundra landscape in northern Sweden. Percentages of (A) total loss of DOC and (B) use of DOC for bacterial production are plotted against the *in situ* share (%) of protein-like fluorescent dissolved organic matter (component 6).

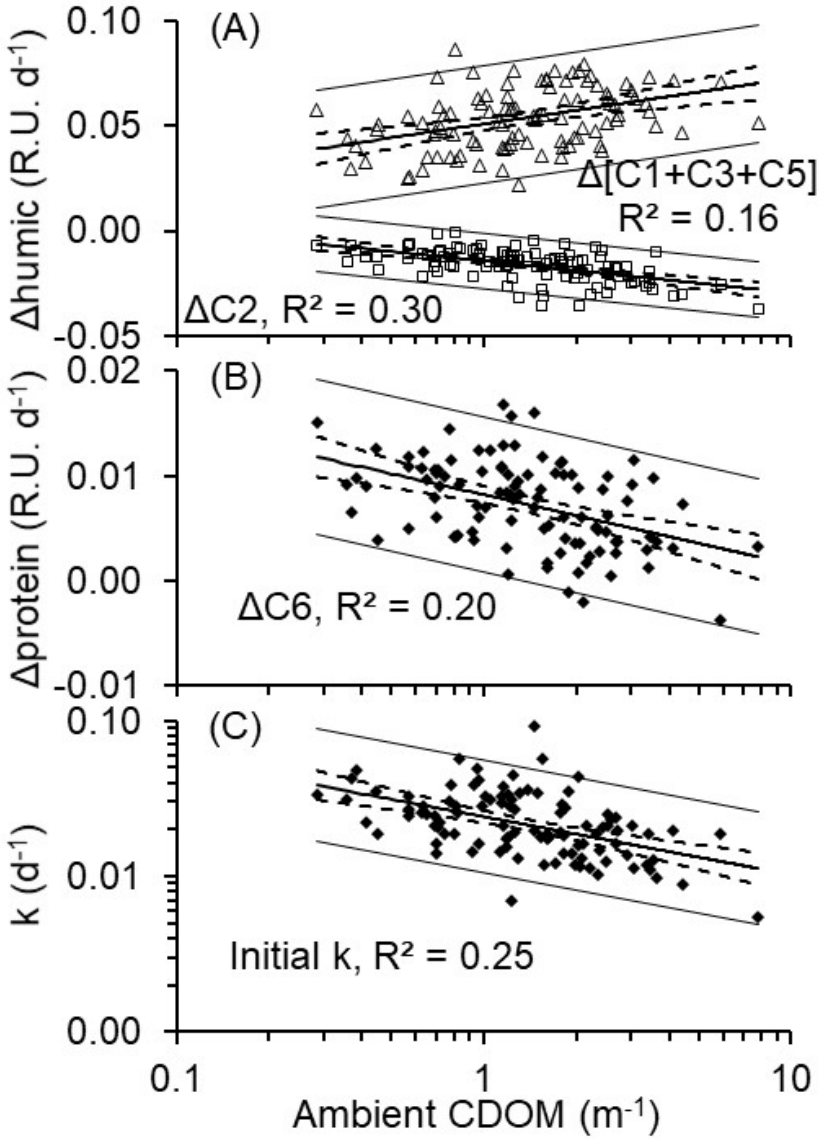

Figure 4. (A-B) Incubation changes in fluorescence components and in (C) initial decay coefficients k regressed from colored dissolved organic matter at 440 nm (CDOM). Dashed lines show 95% CI of the regressions. Observations are 95% likely to fall between the outer upper and lower lines running parallel with the regression lines.

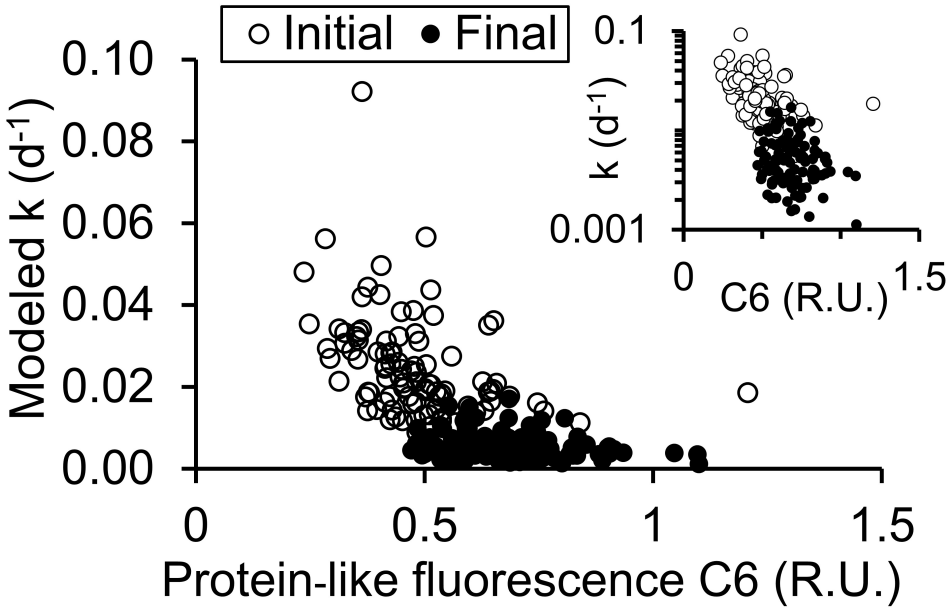

Figure 5. Modeled decay coefficient k plotted against the absolute concentration of protein-like fluorescence C6 at the initial and final stage of 28-day dark laboratory incubations of water from 101 Swedish tundra lakes. The insert figure shows the same data, but on a logarithmic y-axis scale.